06.5;08.2

Defect structure of α-Ga_2O_3 film grown on a *m*-face sapphire substrate, according to transmission electron microscopy investigation

© A.V. Myasoedov[1], I.S. Pavlov[2], A.I. Pechnikov[1,3], S.I. Stepanov[1,3], V.I. Nikolaev[1,3]

[1] Ioffe Institute, St. Petersburg, Russia
[2] Shubnikov Institute of Crystallography „Crystallography and Photonics", Russian Academy of Sciences, Moscow, Russia
[3] Perfect Crystals LLC, Saint-Petersburg, Russia
E-mail: amyasoedov88@gmail.com

Received September 14, 2022
Revised November 9, 2022
Accepted November 14, 2022

The results of a study by transmission electron microscopy of the structural state of α-Ga_2O_3 film with a thickness of about 1 micron, grown on the prismatic *m*-face sapphire by the method of chloride vapor phase epitaxy, are presented. The influence of the substrate orientation on the formation of the dislocation structure is discussed. Threading dislocations, including those with the Burgers vector $1/3\langle 11\bar{2}0\rangle$, and dislocation half-loops are revealed. The inclined propagation of dislocations and the formation of dislocation half-loops result in the reduction of the threading dislocation density near the surface..

Keywords: dislocations, gallium oxide, TEM.

DOI: 10.21883/TPL.2023.01.55353.19365

Ultra-wide-gap semiconductor Ga_2O_3 is a promising material for power and optoelectronic devices [1]. Both thermally stable polymorph β-Ga_2O_3 with a monoclinic structure [2] and metastable phases of gallium oxide [3,4] are of interest. Specifically, α-Ga_2O_3 with a corundum structure has the widest bandgap ($E_g = 5.3$ eV) of all the polymorphic modifications. Layers of α-Ga_2O_3 are normally grown on the basal face of a sapphire substrate, where the layer and the substrate are strongly mismatched in parameter a ($\Delta a/a \sim 4.7\%$). A high density of threading dislocations (TDs), which penetrate the layer from the interface with the substrate to the surface, is established in the layer as a result [5–7]. The following approaches are used to reduce the TD density in epitaxial α-Ga_2O_3 layers: masking of substrates [8], growth on patterned substrates [9], and the deposition of buffer layers [10]. The use of prismatic and pyramidal faces of sapphire is an alternative to these approaches [11–13].

Crystals of gallium oxide with a corundum structure belong to the trigonal crystal system (space group $R\bar{3}c$). The hexagonal coordinate system with lattice cell parameters $a_0 = 4.9825$ Å and $c_0 = 13.433$ Å is used to characterize α-Ga_2O_3. Films deposited onto the basal face of sapphire retain the substrate orientation: $(0001)_{\alpha\text{-}Ga_2O_3} \parallel (0001)_{sapphire}$ and $[10\bar{1}0]_{\alpha\text{-}Ga_2O_3} \parallel [10\bar{1}0]_{sapphire}$ [14]; directions type $\langle 10\bar{1}0\rangle$ are equivalent in this case. If a film is grown on the prismatic *m*-face of sapphire, the orientation relations remain the same, but directions type $\langle 10\bar{1}0\rangle$ become non-equivalent. One direction (we denote it as $[1\bar{1}00]$) coincides with the growth direction, while the other two do not. A $\sim 3.3\%$ mismatch in lattice parameter c between the layer and the substrate in the interface plane is another important feature of epitaxy of α-Ga_2O_3 on the *m*-face of sapphire.

In the present study, an α-Ga_2O_3 film grown on the prismatic *m*-face of sapphire is considered. The results of examination of its structural state by transmission electron microscopy (TEM) are reported, and the influence of the substrate orientation on the formation of the dislocation structure is discussed.

Epitaxial α-Ga_2O_3 films were fabricated by chloride vapor phase epitaxy at a temperature of 500°C and atmospheric pressure in a horizontal quartz reactor produced at Perfect Crystals LLC [4]. An Osiris transmission/scanning electron microscope (ThermoFisher Scientific, USA) at accelerating voltage of 200 kV was used to study the crystal structure defects.

Two mutually perpendicular cross sections of the sample were prepared for TEM studies in order to characterize the dislocation structure emerging in an epitaxial film as a result of mismatch in lattice parameters a and c in the interface plane. These sections were used to probe the vicinity of zone axes [0001] and $[11\bar{2}0]$. The review of slip systems in α-Al_2O_3 [15] allows one to choose the most probable Burgers vectors of dislocations that should emerge in an α-Ga_2O_3 film in the process of stress relaxation of mismatch strain. Specifically, stress induced by a mismatch in parameter a is likely to relax through the formation of mismatch dislocations with Burgers vector $\pm 1/3\langle 11\bar{2}0\rangle$ and the corresponding TDs (Fig. 1, *a*). As for a mismatch in parameter c, the most likely way of stress relaxation is the emergence of mismatch dislocations with Burgers vector $\langle hkil\rangle$ with $l \neq 0$ (e.g., $\pm 1/3\langle 1\bar{1}01\rangle$) and the corresponding TDs (Fig. 1, *b*).

The extinction condition $\mathbf{g} \cdot \mathbf{b} = 0$, where $\mathbf{g}$ is the diffraction vector corresponding to the acting reflection and $\mathbf{b}$ is the Burgers vector, may be applied in the study of

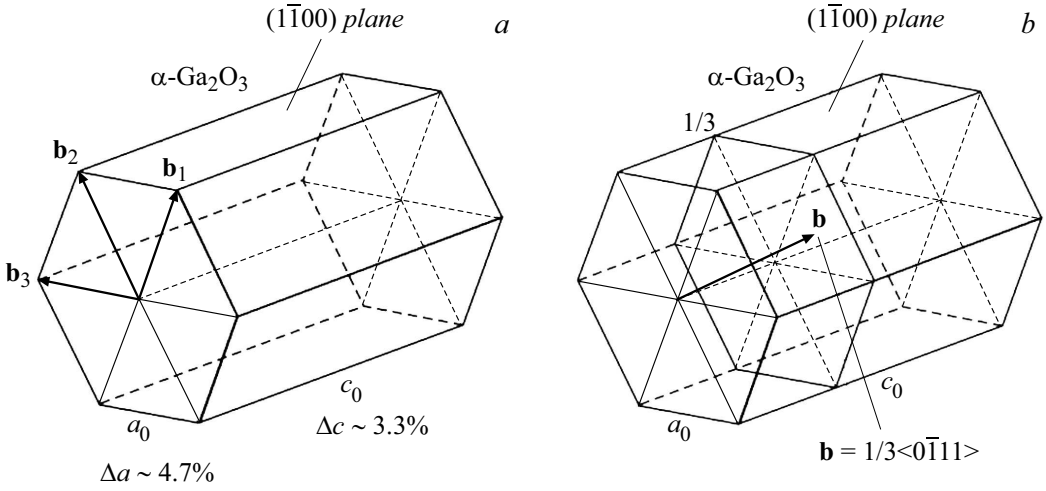

Figure 1. Schematic diagrams of Burgers vectors of TDs and mismatch dislocations, which presumably emerge upon relaxation of stress of mismatch strain, for a mismatch in lattice parameters a (a) and c (b) in growth of α-Ga_2O_3 films on the m-face of sapphire.

Table of scalar products $\mathbf{g} \cdot \mathbf{b}$ used to determine the Burgers vector based on the dislocation extinction condition [16]

b	$\mathbf{g} = 3\bar{3}00$	$\mathbf{g} = 30\bar{3}0$	$\mathbf{g} = 0\bar{3}30$	$\mathbf{g} = 11\bar{2}0$	$\mathbf{g} = 2\bar{1}\bar{1}0$	$\mathbf{g} = 1\bar{2}10$	$\mathbf{g} = 0006$
$\pm 1/3[11\bar{2}0]$	0	± 3	∓ 3	± 2	± 1	∓ 1	0
$\pm 1/3[1\bar{2}10]$	± 3	0	± 3	∓ 1	± 1	± 2	0
$\pm 1/3[\bar{2}110]$	∓ 3	∓ 3	0	∓ 1	∓ 2	∓ 1	0
$\pm 1/3[1\bar{1}01]$	± 2	± 1	± 1	0	± 1	± 1	± 2
$\pm 1/3[01\bar{1}1]$	± 1	∓ 1	± 2	∓ 1	0	± 1	± 2
$\pm 1/3[10\bar{1}1]$	± 1	± 2	∓ 1	± 1	± 1	0	± 2

dislocations imaged by TEM in cross sections of samples. Residual contrast induced by the term dependent on the angle between $\mathbf{g}$ and cross product $\mathbf{b} \times \mathbf{l}$, where $\mathbf{l}$ is a unit tangent vector to the dislocation line, may be detected for an edge dislocation. The table of dot products $\mathbf{g} \cdot \mathbf{b}$, where vectors $\mathbf{g}$ and $\mathbf{b}$ correspond to observable reflections and the chosen Burgers vectors of dislocations, respectively, was complied in accordance with the procedure outlined in [16].

It can be seen from Fig. 2 that the film has a uniform thickness of $\sim 1\,\mu$m is the region of observation. The results of examination of the electron microdiffraction pattern confirmed that the grown film belongs to the α-phase and has the same orientation as the substrate.

Figure 2, *a* shows dark-field images of one and the same sample region observed around the zone axis [0001] for reflections $3\bar{3}00$, $0\bar{3}30$, and $30\bar{3}0$. The behavior of dislocations differs considerably from the one found in films with a similar crystal structure grown on the standard c-face of sapphire, which typically feature dense arrays of strictly vertical TDs with virtually zero interaction between them [5–7]. All three images for reflections $3\bar{3}00$, $0\bar{3}30$, and $30\bar{3}0$ reveal similar dislocation structure patterns: almost vertical straight TDs with inclined sections and dislocation half-loops. Certain configurations are indicative of the interaction of dislocations that results in both merging and splitting relative to the growth direction. Dislocation lines with banded contrast are inclined relative to the image plane. This is confirmed by the images of the perpendicular cross section prepared for examination within the axis of zone $[11\bar{2}0]$. These images of the film are presented in Fig. 2, *b*.

In order to reveal dislocations with Burgers vector $1/3\langle 11\bar{2}0\rangle$ (see the table) in dark-field images for reflections $3\bar{3}00$, $0\bar{3}30$, and $30\bar{3}0$, one needs to search for such dislocations that have zero or weak contrast for one of the reflections and are clearly visible in the other two reflections. The contrast of dislocation lines *1* in Fig. 2, *a* vanishes in reflection $30\bar{3}0$. At the same time, they are seen clearly in reflections $3\bar{3}00$ and $0\bar{3}30$. Dislocation lines *2* are invisible in reflection $0\bar{3}30$, but are seen in reflections $3\bar{3}00$ and $30\bar{3}0$. Thus, dislocations denoted as *1* and *2* have Burgers vectors $\mathbf{b}_1 = \pm 1/3[1\bar{2}10]$ and $\mathbf{b}_2 = \pm 1/3[\bar{2}110]$. Vectors $\mathbf{b}_1$ and $\mathbf{b}_2$ correspond (except for sign) to the vectors indicated in the diagram in Fig. 1, *a*. Note that the projections of dislocations *1* and *2* typically deflect to the right and to the left of the growth direction near the layer surface. This should enhance their screw components. Only a small fraction of identified dislocations are denoted by numbers *1* and *2* in Fig. 2.

Dislocations with Burgers vectors $\mathbf{b}_3 = \pm 1/3[11\bar{2}0]$, which should have zero contrast in reflection $3\bar{3}00$, were not detected directly. Apparently, these dislocations lie in pyramidal planes: this assumption is supported indirectly by

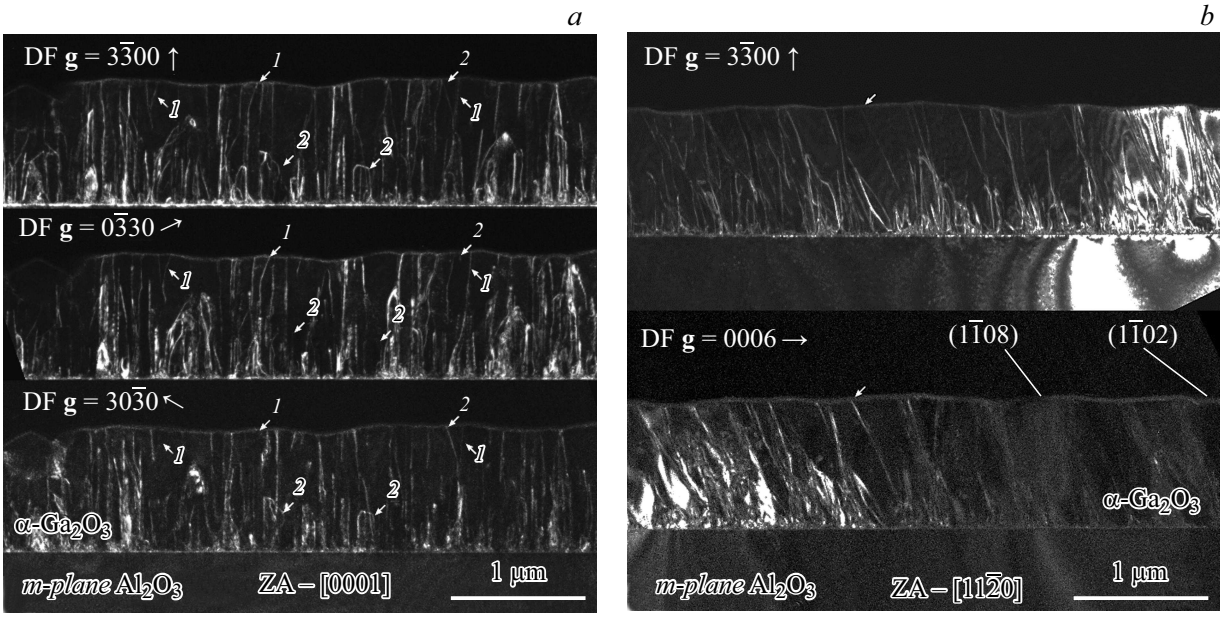

Figure 2. Dark-field TEM images of one and the same region for reflections 3$\bar{3}$00, 0$\bar{3}$30, and 30$\bar{3}$0 observed around the axis of zone [0001] (*a*) and one and the same region for reflections 3$\bar{3}$00 and 0006 observed around the axis of zone [11$\bar{2}$0] (*b*).

the images for the perpendicular cross section. If this is the case, their contrast does not vanish due to term $\mathbf{g} \cdot (\mathbf{b} \times \mathbf{l})$.

The same is true for dislocations with Burgers vector $1/3\langle 1\bar{1}01\rangle$. Therefore, TEM images for reflections 11$\bar{2}$0, 2110, and 1$\bar{2}$10 in observations around the axis of zone [0001] are not shown.

Figure 2, *b* presents the TEM images for reflections 3$\bar{3}$00 and 0006 obtained for the second cross section in observations around the zone axis [11$\bar{2}$0]. Just as for the previous orientation, all dislocations with Burgers vectors other than $1/3[11\bar{2}0]$ should be observed in reflection 3$\bar{3}$00. Only dislocations $\langle hkil\rangle$ with $l \neq 0$ should remain in contrast in reflection 0006, but such dislocations were not detected directly. It can be seen that all dislocations observed in reflection 3$\bar{3}$00 vanished in reflection 0006 (region on the right). The diffraction conditions are not completely satisfied for the region on the left. This is attributable to a lamella bend, which is corroborated by the observation of bend contours on the substrate.

It follows from the image for reflection 3$\bar{3}$00 in this orientation that the overwhelming majority of dislocations are inclined. An example of an inclined dislocation is denoted with an arrow in Fig. 2, *b*. The inclination is well-pronounced and is likely to be induced be the crystal structure of the film. In the present case, the electron microdiffraction pattern for the axis of zone [11$\bar{2}$0] indicates that planes (1$\bar{1}$02) and (1$\bar{1}$08), which are shown schematically in Fig. 2, *b*, correspond to a similar TD inclination in this geometry, while, e.g., (1$\bar{1}$0$\bar{4}$) corresponds to the opposite inclination. Thus, it was found that TD lines propagate primarily along pyramidal planes with an inclination close to plane (1$\bar{1}$08).

A TEM study of the structural state of a film of gallium oxide of the α-phase grown on the prismatic *m*-face of sapphire was carried out. The aim of this study was to characterize the dislocation structure with the mismatch in lattice parameters *a* and *c* taken into account. Having analyzed the diffraction contrast at dislocations for different acting reflections, we found that the overwhelming majority of dislocations have a Burgers vector type $1/3\langle 11\bar{2}0\rangle$. TD lines propagate primarily along pyramidal planes with an inclination close to plane (1$\bar{1}$08). TDs propagating along basal plane (0001) are less widespread. The presence of a large number of dislocation half-loops and reactions of interaction between dislocations was noted. This facilitates a several-fold reduction in their density in the direction from the interface to the surface.

Funding

This study was supported financially by grant No. 19-29-12041 mk from the Russian Foundation for Basic Research.

Conflict of interest

The authors declare that they have no conflict of interest.

References

[1] Y. Yuan, W. Hao, W. Mu, Z. Wang, X. Chen, Q. Liu, G. Xu, C. Wang, H. Zhou, Y. Zou, X. Zhao, Z. Jia, J. Ye, J. Zhang, S. Long, X. Tao, R. Zhang, Y. Hao, Fundam. Res., **1** (6), 697 (2021). DOI: 10.1016/j.fmre.2021.11.002

[2] Y. Tomm, P. Reiche, D. Klimm, T. Fukuda, J. Cryst. Growth, **220** (4), 510 (2000). DOI: 10.1016/S0022-0248(00)00851-4

[3] T. Oshima, T. Nakazono, A. Mukai, A. Ohtomo, J. Cryst. Growth, **359** (1), 60 (2012). DOI: 10.1016/j.jcrysgro.2012.08.025
[4] A.I. Pechnikov, S.I. Stepanov, A.V. Chikiryaka, M.P. Scheglov, M.A. Odnobludov, V.I. Nikolaev, Semiconductors, **53** (6), 780 (2019). DOI: 10.1134/S1063782619060150.
[5] T.C. Ma, X.H. Chen, Y. Kuang, L. Li, J. Li, F. Kremer, F.-F. Ren, S.L. Gu, R. Zhang, Y.D. Zheng, H.H. Tan, C. Jagadish, J.D. Ye, Appl. Phys. Lett., **115** (18), 182101 (2019). DOI: 10.1063/1.5120554
[6] Y. Oshima, S. Yagyu, T. Shinohe, J. Cryst. Growth, **576**, 126387 (2021). DOI: 10.1016/j.jcrysgro.2021.126387
[7] K. Kaneko, H. Kawanowa, H. Ito, S. Fujita, Appl. Phys., **51** (2R), 020201 (2012). DOI: 10.1143/JJAP.51.020201
[8] Y. Oshima, K. Kawara, T. Shinohe, T. Hitora, M. Kasu, S. Fujita, APL Mater., **7** (2), 022503 (2019). DOI: 10.1063/1.5051058
[9] V.I. Nikolaev, A.I. Pechnikov, L.I. Guzilova, A.V. Chikiryaka, M.P. Shcheglov, V.V. Nikolaev, S.I. Stepanov, A.A. Vasil'ev, I.V. Shchemerov, A.Ya. Polyakov, Tech. Phys. Lett., **46** (3), 228 (2020). DOI: 10.1134/S106378502003013X.
[10] R. Jinno, T. Uchida, K. Kaneko, S. Fujita, Appl. Phys. Express, **9** (7), 071101 (2016). DOI: 10.7567/APEX.9.071101
[11] S. Shapenkov, O. Vyvenko, V. Nikolaev, S. Stepanov, A. Pechnikov, M. Scheglov, G. Varygin, Phys. Status Solidi B, **259** (2), 2100331 (2022). DOI: 10.1002/pssb.202100331
[12] Y. Cheng, Y. Xu, Z. Li, J. Zhang, D. Chen, Q. Feng, S. Xu, H. Zhou, J. Zhang, Y. Hao, C. Zhang, J. Alloys Compd., **831**, 154776 (2020). DOI: 10.1016/j.jallcom.2020.154776
[13] K. Akaiwa, K. Ota, T. Sekiyama, T. Abe, T. Shinohe, K. Ichino, Phys. Status Solidi A, **217** (3), 1900632 (2020). DOI: 10.1002/pssa.201900632
[14] Y. Oshima, E.G. Víllora, K. Shimamura, Appl. Phys. Express, **8** (5), 055501 (2015). DOI: 10.7567/APEX.8.055501
[15] J.D. Snow, A.H. Heuer, J. Am. Ceram. Soc., **56** (3), 153 (1973). DOI: 10.1111/j.1151-2916.1973.tb15432.x
[16] P.B. Hirsch, A. Howie, R.B. Nicholson, D.W. Pashley, M.J. Whelan, *Electron microscopy of thin crystals* (Butterworths, London, 1965).